

# Let's Hope it Works!

## Inaccurate Supervision of Neural Networks with Incorrect Labels: Application to Epilepsy

Florian Dubost<sup>1,\*</sup>, Erin Hong<sup>1,\*</sup>, Daniel Y Fu<sup>1</sup>, Nandita Bhaskhar<sup>1</sup>, Siyi Tang<sup>1</sup>, Khaled Saab<sup>1</sup>, Daniel Rubin<sup>1</sup>, Jared Dunnmon<sup>1</sup>, and Christopher Lee-Messer<sup>1</sup>

Stanford University, Stanford, U.S.

**Abstract.** This work describes multiple weak supervision strategies for video processing with neural networks in the context of epilepsy. To study seizure onset, researchers have designed automated methods to detect seizures from electroencephalography (EEG), a modality used for recording electrical brain activity. However, the EEG signal alone is sometimes not enough for existing detection methods to discriminate seizure from artifacts having a similar signal on EEG. For example, such artifacts could be triggered by patting, rocking or suctioning in the case of neonates. In this article, we addressed this problem by automatically detecting an example artifact—patting of neonates—from continuous video recordings of neonates acquired during clinical routine. We computed frame-to-frame cross-correlation matrices to isolate patterns showing repetitive movements indicative of patting. Next, a convolutional neural network was trained to classify whether these matrices contained patting events using weak training labels — noisy labels generated during normal clinical procedure. The labels were considered weak as they were sometimes incorrect. We investigated whether networks trained with more samples, containing more uncertain and weak labels, could achieve a higher performance. Our results showed that, in the case of patting detection, such networks could achieve a higher recall and focused on areas of the cross-correlation matrices that were more meaningful to the task, without sacrificing precision.

**Keywords:** video, epilepsy, seizure, weak labels, incorrect labels

## 1 Introduction

Epilepsy is one of the most common neurological disorders, affecting 50 million people worldwide [1]. Patients with epilepsy have chronic seizures, which are episodes in which the subject experiences involuntary movements and sometimes even loses consciousness. With a risk of premature death three times higher than that of the general population, patients with epilepsy experience socio-economic

---

\* indicates equal contribution

burdens in addition to facing the unpredictability and frequency of seizure onset [3]. By monitoring patients at-risk, doctors can make more meaningful therapeutic decisions.

As continuous monitoring of patients creates vast amounts of data, and observation is extremely time-consuming, researchers have developed methods to automatically detect seizures relying on electroencephalographic (EEG) data [4, 5]. However, some EEG artifacts can resemble seizure activity, and mislead automated methods. For example, the physical patting that occurs when clinicians care for their neonatal patients can produce a seizure-like EEG signal, resulting in false positive classifications. To discard such false positives, some hospitals also record video data in addition to the continuous EEG monitoring of their patients. Doctors subsequently need to manually review these videos, which is time-consuming, as each patient generates hours of video data each day. In this work, we propose an automated method to detect patting from continuous video recordings of neonates. To the best of our knowledge, it is the first time that continuous video recordings from clinical routine are leveraged to improve automated seizure detection methods.

We computed frame-to-frame cross-correlation matrices over five seconds long video segment to highlight checkerboard patterns indicative of the repetition of the patting movements. Dwibedi et al. [6] also used cross-correlation matrices to analyze repetitive motion, and focused on the estimation of the number of repetitions. In our data, the detection of repetitive motion could be more challenging than in the data of Dwibedi et al. [6], as there was more noise in the hospital videos, such as occlusion of the patients by either relatives or nurses, occlusion by bed sheets, and busy hospital background. Contrary to Dwibedi et al. [6], we did not attempt to count the patting repetitions, and instead detected the start and end times of the patting through longer video sequences.

The cross-correlation matrices were weakly labelled in our approach: to speed up the labelling process, only the beginnings of the patting sequences were labelled by clinicians during the clinical routine. We sampled short videos segment following this label and considered them positives–patting–without knowing the end of the patting sequence. The further away the segments were sampled from the labelled times, the more they risked to be negative samples. By varying the sampling distance away from the labelled start time of patting, we could vary the probability of the sampled segment to be a true positive, hence varying the quality of its label. We trained two neural networks with such labels: a conservative network, which only used samples following the originally labelled patting times, and a risk tolerant network, which used more samples, further from the original patting times, hence with weaker and more uncertain labels. The rest of this article details both approaches and compares their results, using precision-recall curves, area under the receiver operating characteristic curve, F1-score, and computation of network’s attention.

Zhou et al. [7] also employed the wording *weak label* to describe partially incorrect labels such as the ones used in this work, which they described as *inaccurate supervision*. The authors completed their taxonomy of weak labels by

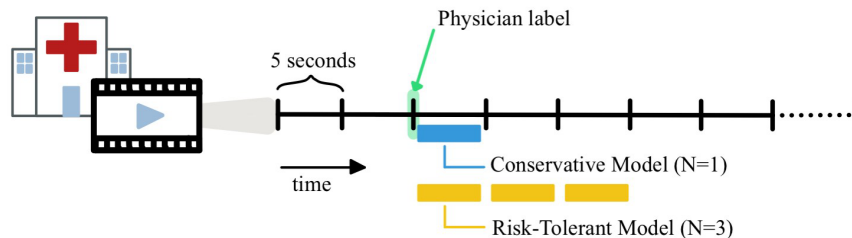


**Fig. 1.** Sampling of the video segments.

adding the categories *incomplete supervision*—also called *semi-supervised*—and *inexact supervision*. The works of Hao et al. [9] and Karimi et al. [10] are other examples of inaccurate supervision with deep learning for medical data. More generally, inaccurate supervision is more frequently found in medical image analysis than in computer vision, as the diagnosis or quantification of medical images is observer-dependent. Crowd-sourcing [11, 12] is another example of inaccurate supervision. A large group of individuals, with varying levels of skill and care, label a dataset, which often leads to having multiple labels per sample. In our patting videos, there is however always a single label for a given time.

## 2 Methods

### 2.1 Dataset

The dataset consisted of 294 video recordings acquired during continuous monitoring of patients as part of the clinical routine of the Lucile Packard Children’s Hospital. The recordings lasted between 99 seconds and 720 minutes with a median of 33 minutes. As part of the clinical routine, these videos recordings were labelled by clinicians for patting sequences with the corresponding start time only. In the rest of this article, these labels will be called *weak labels*. 28 of the 294 videos, recorded from 26 patients, were reviewed a second time, and both the beginning and the end the patting sequence were labelled. We call these labels *strong labels*. The strong labels encompassed 2214 seconds of patting in total. The set of 28 videos with strong labels was split randomly into three subsets using stratified sampling over the number of patting seconds: the training set, 14 videos, the validation set, 4 videos, the test set, 10 videos. The training, validation and test videos were also separated by patient. The rest of the dataset, 399 weak labels from 266 videos from 224 other patients, were used in the training set only. The models were optimized using the training and validation set, while the test set was set aside for independent evaluation.

Five second long video segments, sampled at 15 frames per seconds, were extracted from the videos. The length of the sampled video segments is discussed

in the discussion section. For the training and validation sets, non-overlapping positive (patting) segments were sampled to cover the patting time indicated by the strong labels. Negative segments were sampled from the rest of the recording at random. For the weak labels,  $N$  non-overlapping consecutive positive segments were sampled after the labelled times (Figure 1). The further away—and the higher  $N$ —a positive was sampled from the original weak label time, the less likely it was to correspond to an actual patting sequence, and the weaker its label was considered. This is further detailed in the following section. Weak negative segments were sampled at random, 5 minutes away from the weak label times. To evaluate the models on the test set, consecutive non-overlapping video segments were extracted to span the full video time.

## 2.2 Risk Estimation

We estimated the probability of a weak sample to be incorrect using the following formula:

$$P(x) = 1 - e^{-\alpha x} \quad (1)$$

where  $\alpha$  is a calibration factor and  $x$  is the number of seconds at which the video segment is sampled after the originally labelled time. Following the definition of number of sampled consecutive non-overlapping segments  $N$ ,  $x$  could only take a set of discrete values such as  $x = nL$ , where  $L$  is the length of sampled segments in seconds, and  $n \in \{1, \dots, N\}$  is the number of segments after the originally labelled time.

The probability of having an incorrect label in a sequence of  $N$  segments sampled from a single labelled time is consequently

$$\frac{1}{N} \sum_{n=0}^{N-1} P(nL) = \frac{1}{N} \sum_{n=0}^{N-1} 1 - e^{-\alpha nL} = 1 - \frac{1}{N} \sum_{n=0}^{N-1} e^{-\alpha nL} \quad (2)$$

For a series of  $T$  weak label times the probability of having an incorrect label becomes

$$\frac{1}{T} \sum_{t=1}^T \frac{1}{N_t} \sum_{n=0}^{N-1} P(nL) \quad (3)$$

where  $N_t$  is the number of segments sampled for time  $t$ . If the same number of segment  $N$  is sampled for each labelled times, as in our experiments, this can be simplified as

$$P_{\alpha,L}(N) = \frac{1}{TN} \sum_{t=1}^T \sum_{n=0}^{N-1} P(nL) = \frac{1}{N} \sum_{n=0}^{N-1} P(nL) = 1 - \frac{1}{N} \sum_{n=0}^{N-1} e^{-\alpha nL} \quad (4)$$

The probability  $P_{\alpha,L}(N)$  can be used to estimate the level of risk taken by a model trained with such a dataset. Figure 2 compares such risk levels as a function of the number of consecutive samples  $N$  with varying calibration levels  $\alpha$  and segment lengths  $L$ .

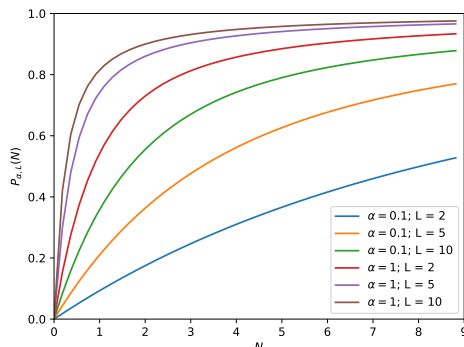


**Fig. 2.** Comparison risk levels  $P_{\alpha,L}(N)$  as a function of the number of consecutive samples  $N$  with varying calibration levels  $\alpha$  and segment lengths  $L$ . As expected, with a fixed calibration, sampling shorter segments can allow to gather more segments without changing the level of risk of having incorrect labels.

### 2.3 Normalized Cross-Correlation Matrix

A frame-to-frame, hence  $75 \times 75$ , normalized cross-correlation matrix was computed for each video segment. The diagonal from the top left corner to the bottom right corner indicated cross-correlation of the current frame with itself, and displayed consequently the highest values. The top right side of the cross-correlation matrices were set to 0 to avoid repetitive information due to the symmetry of the cross-correlation function. Examples of such matrices are shown in Figure 5. These matrices were normalized in  $[0, 1]$  using their 1st and 99th percentile values. The repetition of the patting movements were expected to be easily detectable as a checkerboard pattern on the cross-correlation matrices.

### 2.4 Weakly Supervised Neural Networks

Both conservative and risk tolerant models had the same architecture. Their input was a single cross-correlation matrix representing a single five second long video segment, and their output was a patting pseudo-probability ranging from 0 to 1. The architecture was similar to that of a small ResNet [13]. The networks had two  $3 \times 3$  convolutional layers, followed by a  $2 \times 2$  max-pooling layer, again two  $3 \times 3$  convolutional layers, a global average pooling layer, and a fully connected layer followed by a sigmoid activation function, combining the contribution of the different features into a single output in  $[0, 1]$ . The first two convolutional layers had 32 filters each, and the last two convolutional layers, 64 filters each. The convolutions were zero-padded and followed by ReLU activations. We used skip connections between the input and output of two successive convolutional layers.

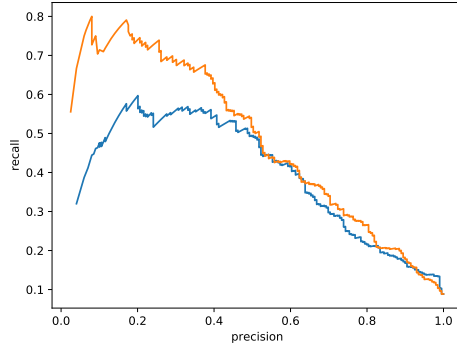


**Fig. 3.** Comparison of the precision-recall curves of the two models. The conservative model is represented in blue, and the risk tolerant model in orange.

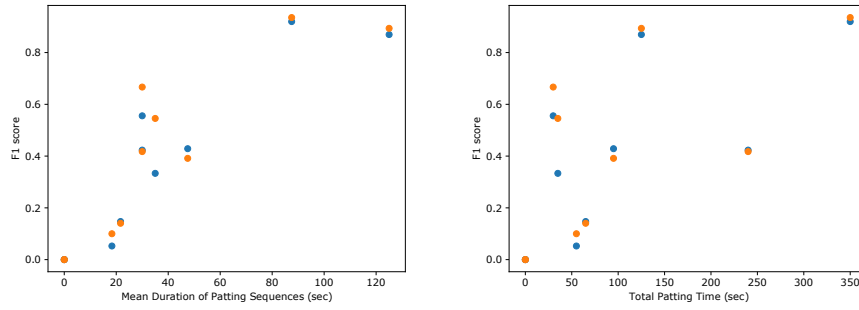


**Fig. 4.** Performance, measured as F1-score, as a function of the average time of patting sequences (left) and total patting time in a video (right) for the 10 videos of the test set. Each dot corresponds to a single video. On the bottom left corner, four dots—two blue and two orange—are overlaid and correspond to videos without patting. The conservative model is represented in blue, and the risk tolerant model in orange. On the left, the Pearson correlation coefficient was 0.87 for the risk tolerant model and 0.91 for the conservative model. On the right, it was 0.63 for the risk tolerant model and 0.71 for the conservative model.

The networks were trained using a weighted-cross entropy loss and Adam optimizer with Keras’ default parameters. The training was stopped after the validation F1-score had not increased for 400 epochs. The best model was selected as the one with maximum F1-score on the validation set.

To ease and accelerate the training, we pretrained the models using the strong labels only. For pretraining, a single model was trained from random weight initialization with as many random negatives as available positives for both the training and validation sets. The conservative model was fine-tuned from this

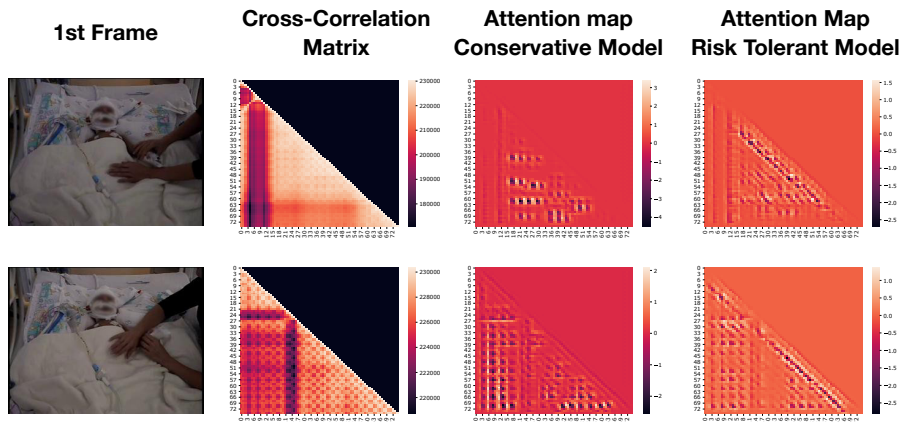


**Fig. 5.** Comparison of the attention maps of the risk tolerant and conservative models for two random positive video segments. The baby’s face has been blurred for privacy.

model using 10 times more negatives than positives, using all available positives from the strong labels, plus 399 ( $N = 1$ ) positives from the weak labels. The risk tolerant model was fine-tuned like the conservative model, with 1197 ( $N = 3$ ) weak positives instead of 399.

## 2.5 Evaluation

**Inspection of Network Attention.** To verify that the networks focused on the repetitive portions (checkerboard) of the cross-correlation matrices, we computed attention maps highlighting areas of the image used for the models’ predictions. Attention maps were computed using guided-backpropagation [14], which computes the derivative of the output with respect to the input, the cross-correlation matrix. Pixels of high absolute value in the attention map correspond to regions used by the network for its prediction.

**Metrics.** We computed evaluation metrics segment-wise on the test set. We reported F1 scores, precision recall curves, areas under the precision-recall curves, and areas under the receiver operating characteristic curves (AUC).

## 3 Results

All metrics are reported in Table 1. Both conservative and risk tolerant models had similar receiver operating characteristic curves and performed better for videos with longer duration of individual patting sequences. Their performance was less correlated to the total patting time in a video (Figure 4). The precision-recall curve (Figure 3) was better for the risk tolerant model. The inspection of the attention maps (Figure 5) revealed that the risk tolerant model focused

more on elements of the cross-correlation matrix that were close to the diagonal, i.e. frames close to each other, while the conservative model attempted to find checkerboard patterns anywhere in the cross-correlation matrices, e.g. at the bottom left corner, which encoded information of frames far apart in time.

## 4 Discussion

We compared two weak supervision approaches for the detection of patting sequences in continuous video recordings from clinical routine. The first approach, the conservative model ( $N = 1$ ), was trained with video segments with more certain labels than the second approach, the risk tolerant model ( $N = 3$ ), which used more samples and with a higher probability of being incorrectly labelled. The risk tolerant model achieved higher recall and focused on areas of the cross-correlation matrices that were more relevant to the task. These results suggest that using additional uncertain—and sometimes incorrect—labels can improve the performance.

Using even more samples with higher probability of being incorrect, e.g.  $N = 4$ , may improve the results further. In addition to the number of positive examples, we hypothesize that the performance of the model depends on the proportion of correctly labelled versus incorrectly labelled positive samples used for training. For example, the performance of the model may be expected to deteriorate when more than half of the positive training samples are incorrectly labelled.

The modelling of risk estimation in Figure 2 showed that, with a fixed calibration, sampling shorter segments would increase the number of video segments without changing the level of risk of having incorrect labels. The segments should be as short as possible to sample a higher number of segments for a fixed level of risk of having incorrect labels, but should be long enough for model to detect the target motion—e.g. patting—in each individual segments. We also experimented with two second long segments, but could not reach a satisfactory performance on the validation set.

One of the limitations of the proposed risk estimation model is that it considers that each of our weak annotation always correctly indicates a true positive. In our experiments, the reviewing of a subset of weak labels for the creation of the strong labels revealed that some of these weak labels were incorrect: no patting was found in the video (Figure 4). According to the risk estimation model, the

Model	AUC	AuPRC	Pearson of F1 score vs. mean length of patting sequence	Pearson of F1 score vs. total patting time
Conservative	0.89	0.39	0.91	0.71
Risk tolerant	0.89	0.49	0.87	0.63

**Table 1.** Summary of the results. AUC is the area under the ROC curve. AuPRC is the area under the precision-recall curve.

conservative model has a risk level  $P_{\alpha,L}(1)$  equal to 0 while it does use some incorrect weak labels. To improve the risk estimation model, one could incorporate a term accounting for the risk of the original weak label to be incorrect.

In this work, only non-overlapping video segments were considered. Sampling overlapping video segment could act as data augmentation, regularize the models, and hopefully improve the performance further. The risk estimation model would consequently need to be adapted.

In terms of application, both conservative and risk tolerant models showed high performance for longer patting sequences, but had a low performance for shorter patting sequences. Shorter patting sequences, with e.g. interruptions, were expected to be more difficult to detect but are less relevant to the application of seizure detection. Only longer sequences are expected to create EEG signals that may resemble that of seizures and mislead the automated models, and consequently need to be detected to filter out potential false positives. Future work will focus on the detection of other artifacts from video data.

## 5 Conclusion

We compared weak supervision strategies for inaccurate supervision in the context of video artifact detection for seizure detection. Our results showed that models using more samples with higher probability of being incorrectly labelled could improve the detection performance. We also proposed a risk estimation model to help choosing the hyperparameters of inaccurately supervised video models.

## References

1. Beghi, E., Giussani, G., Nichols, E., Abd-Allah, F., Abdela, J., Abdelalim, A., Abraha, H.N., Adib, M.G., Agrawal, S., Alahdab, F. and Awasthi, A., 2019. Global, regional, and national burden of epilepsy, 1990–2016: a systematic analysis for the Global Burden of Disease Study 2016. *The Lancet Neurology*, 18(4), pp.357-375.
2. Sirven, J.I., 2015. Epilepsy: a spectrum disorder. *Cold Spring Harbor perspectives in medicine*, 5(9), p.a022848.
3. Neligan, A., Bell, G.S., Johnson, A.L., Goodridge, D.M., Shorvon, S.D. and Sander, J.W., 2011. The long-term risk of premature mortality in people with epilepsy. *Brain*, 134(2), pp.388-395.
4. Fergus, P., Hignett, D., Hussain, A., Al-Jumeily, D. and Abdel-Aziz, K., 2015. Automatic epileptic seizure detection using scalp EEG and advanced artificial intelligence techniques. *BioMed research international*, 2015.
5. Saab, K., Dunnmon, J., Ré, C., Rubin, D. and Lee-Messer, C., 2020. Weak supervision as an efficient approach for automated seizure detection in electroencephalography. *npj Digital Medicine*, 3(1), pp.1-12.
6. Dwibedi, D., Aytar, Y., Tompson, J., Sermanet, P. and Zisserman, A., 2020. Counting Out Time: Class Agnostic Video Repetition Counting in the Wild. In *Proceedings of the IEEE/CVF Conference on Computer Vision and Pattern Recognition* (pp. 10387-10396).

7. Zhou, Z.H., 2018. A brief introduction to weakly supervised learning. *National Science Review*, 5(1), pp.44-53.
8. Zou, K.H., Warfield, S.K., Bharatha, A., Tempany, C.M., Kaus, M.R., Haker, S.J., Wells III, W.M., Jolesz, F.A. and Kikinis, R., 2004. Statistical validation of image segmentation quality based on a spatial overlap index1: scientific reports. *Academic radiology*, 11(2), pp.178-189.
9. Hao, D., Zhang, L., Sumkin, J., Mohamed, A. and Wu, S., 2020. Inaccurate labels in weakly supervised deep learning: Automatic identification and correction and their impact on classification performance. *IEEE Journal of Biomedical and Health Informatics*.
10. Karimi, D., Dou, H., Warfield, S.K. and Gholipour, A., 2020. Deep learning with noisy labels: Exploring techniques and remedies in medical image analysis. *Medical Image Analysis*, 65, p.101759.
11. de Herrera, A.G.S., Schaer, R., Antani, S. and Müller, H., 2016. Using crowdsourcing for multi-label biomedical compound figure annotation. In *Deep Learning and Data Labeling for Medical Applications* (pp. 228-237). Springer, Cham.
12. Cheplygina, V., Perez-Rovira, A., Kuo, W., Tiddens, H.A. and De Bruijne, M., 2016. Early experiences with crowdsourcing airway annotations in chest CT. In *Deep Learning and Data Labeling for Medical Applications* (pp. 209-218). Springer, Cham.
13. He, K., Zhang, X., Ren, S. and Sun, J., 2016. Deep residual learning for image recognition. In *Proceedings of the IEEE conference on computer vision and pattern recognition* (pp. 770-778).
14. Springenberg, J.T., Dosovitskiy, A., Brox, T. and Riedmiller, M., 2015. Striving for simplicity: The all convolutional net. *Proceedings of the International Conference for Learning Representations*.